

Nonlinear Analytic Representation of MJO-like Coherence

Mitchell W. Moncrieff

*Mesoscale and Microscale Meteorology Division,
NCAR, Boulder, Colorado 80307-3000, USA
(moncrief@ucar.edu)*

1. Introduction

Understanding the large-scale effects of atmospheric convection on the MJO is necessary to improve global numerical weather prediction models and climate models, a point that is credent through comprehensive model intercomparisons (e.g., Slingo et al 1996; Sperber et al. 1997), as well as papers in the proceedings of this workshop.

The large-scale effects of organized convection has been little studied, especially from the parameterization perspective. Presented herein is a summary of Moncrieff (2003; hereafter M03), to which the reader is referred for a full description of the analytic theory, evaluation against numerically simulated systems and arising issues.

In the MJO distinct scales of convective organization tend to interlock. Figure 1 shows westward-traveling cloud clusters of frequency about 2 days and about 100-km in horizontal scale embedded within eastward-traveling envelopes of large-scale super-clusters a few 1000 km in spatial scale and frequency of about 10 days as described by the analysis of out-going long-wave radiation measurements (Nakazawa 1988).

Early models of the MJO focused on the linear steady response to tropical heating (i.e., Matsuno 1966; Webster 1972; Gill 1980) representing the barotropic response to a prescribed stationary heat source on an equatorial beta-plane. However, the solutions tend to be sensitive to the Newtonian damping applied to realize steady solutions. None of these theories accounts for the mesoscale organization of convection.

The nonlinear steady models of coupled organized dynamics presented herein and in M03 differ deeply from the linear-wave models. These nonlinear models, along with recent multiscale perturbation models (e.g., Sobel et al. 2001; Majda and Klein 2003), provide a physically based systematic framework for quantifying the dynamics of the MJO in particular and convectively-coupled tropical waves in general.

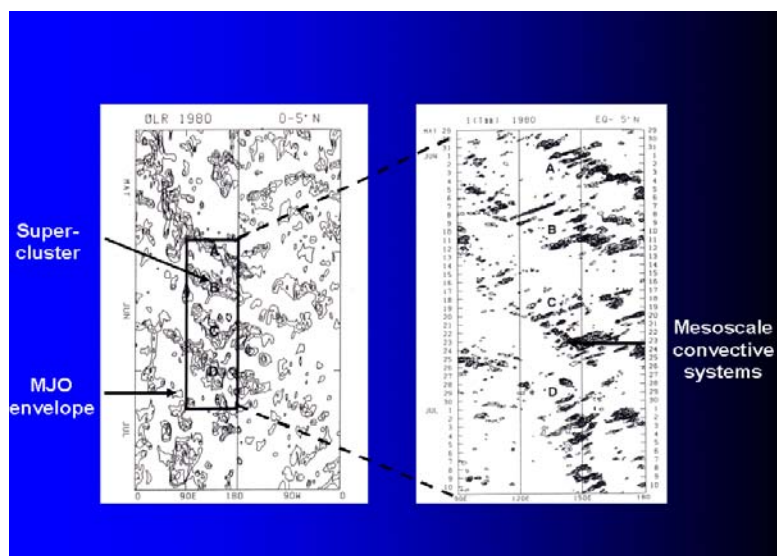


Figure 1: Mesoscale systems, super-clusters and the MJO envelope, [Nakazawa (1988)].

2. Large-scale organization of convection

2.1. Numerically simulated organization

Grabowski (2001; hereafter G01), as well as his paper in this workshop proceeding, reports results of two-dimensional cloud-system-resolving numerical models embedded within a highly idealized coarse-mesh global aqua-planet model. This so-called “cloud-resolving convection parameterization” or “super-parameterization” approach, which takes the place of conventional parameterizations of convection and convection-related processes, is referred to herein simply as *explicit convection* or *the explicit approach*.

For computational reasons, the grid-resolution of the cloud-system models applied in G01 is coarser than ideal (3.5 km). It follows that convective processes on scales of several tens of kilometers are resolved but cumulonimbus convection and small-scale cumulus are not. Presumably, these processes are aliased onto the resolved scales producing distorted convective organization. This *surrogate behavior* produces model bias (Moncrieff and Klinker 1997; M04) for which no cure has been identified. Also, the cloud-system computational domains span just 200 km of the 1250 km coarse-mesh grid: a scale-gap exists but this problem is easily addressed. It follows that G01’s explicit approach represents *convection organized on meso-beta scales* (i.e., 20 km - 200 km) rather than convection *per se*.

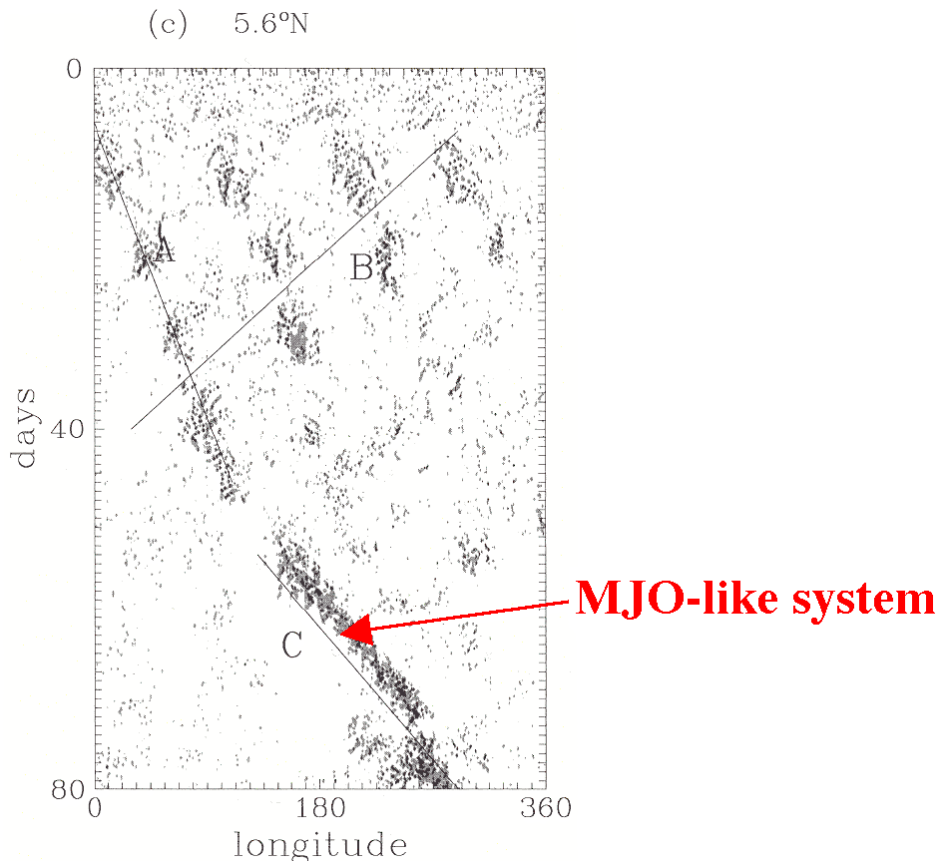


Figure 2: The MJO-like system in G01

2.2. Coupled analytic model

The vertical transport of horizontal momentum, a quantity notoriously prone to misrepresentation, derived from the Moncrieff (1992; hereafter M92) nonlinear model was verified against observations by LeMone and Moncrieff (1993). It follows that the M92 model is a verified ‘transport module’ but not a parameterization of organized convection because the transport module was not coupled to the environment. Herein, an

analytic extension of the M92 model of organized convection, schematized in Fig. 2, is derived, which couples the mesoscale dynamics and large-scale β -plane dynamics. This analytic convection-environment coupling is based on a remarkable analogy between the vorticity dynamics of MJO-like systems on an equatorial beta-plane and organized convection. The formal analogy turns the M92 transport module into an *analytic mesoscale parameterization* of organized convection. The coupled model is based on intuitive physical reasoning that makes powerful nonlinear Lagrangian conservation properties of steady finite-amplitude motion mathematically tractable.

3. Analysis of the simulated large-scale organization of convection

Figure 3 shows that during days 50-80 of G01's highly-idealized aqua-planet simulation, an envelope of convection propagates eastward at about 8 ms^{-1} : the MJO-like system. Asymmetry in the horizontal and vertical directions is key to the organized momentum transport. Figure 4a shows the horizontal structure of 20-day averaged zonal flow in the lower troposphere (2 km) and upper troposphere (12 km) as well as the corresponding vorticity. Large-scale circulations in the lower- and upper-troposphere have distinct physical origins. M03 showed that the large-scale circulation in the lower troposphere is Rossby-gyre-like. In the upper-troposphere the zonal flow is driven by (divergent) outflow from the organized convection in the neighborhood of the Equator.

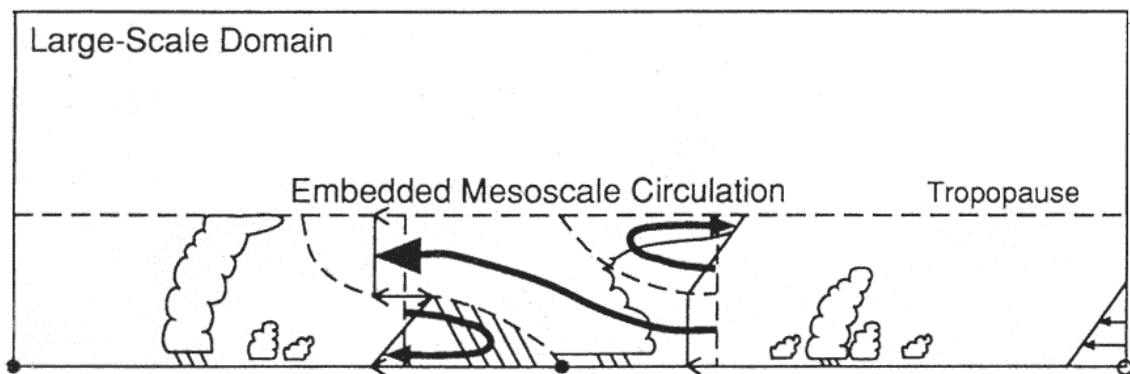
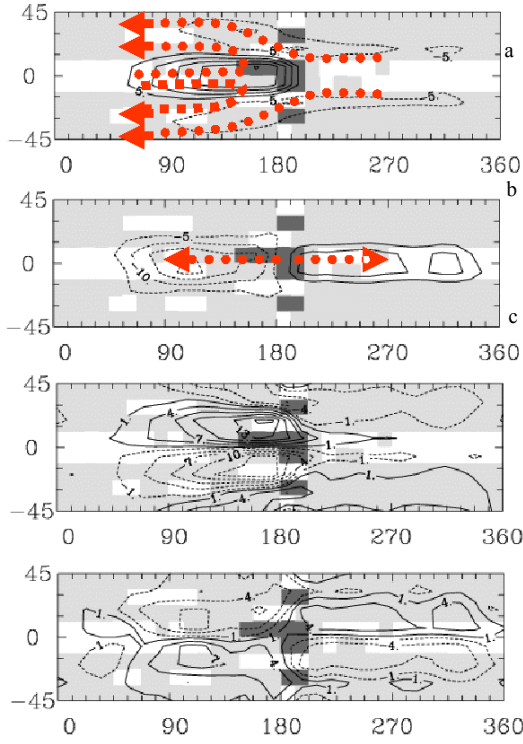


Figure 3: Schema of organized convection represented by the M92 archetypal model.

Figure 4 shows an extensive rearward-directed flow, a weak forward-directed overturning flow and strong surface flow (westerly wind burst) to the rear. The surface pressure falls in the rain area. The large-scale airflow in the horizontal plane in Fig 4b is morphologically similar to the airflow in the vertical plane (Fig. 4). The latter represents the collective effects of organized convection on the meso- β -scale, classically defined as the 20 km- 200 km range of scales.

Horizontal structure



Vertical structure

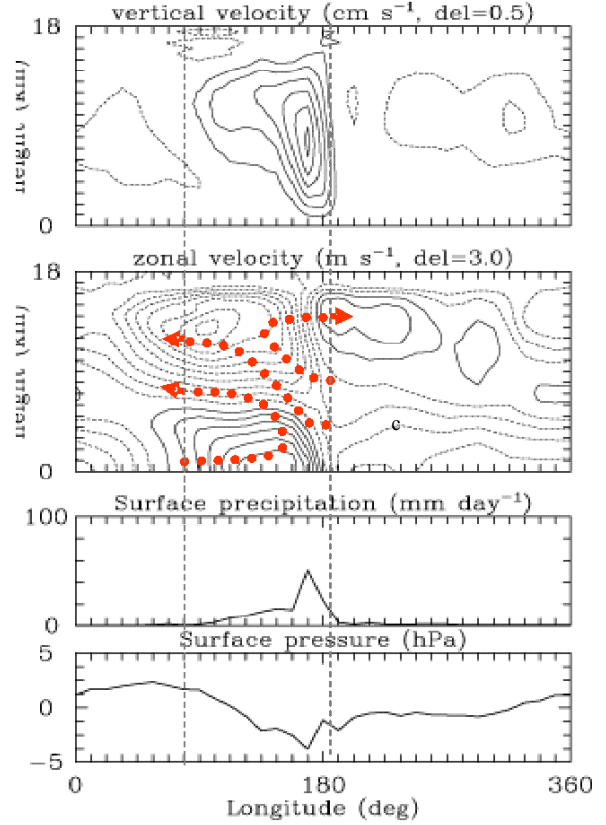


Figure 4: Left, 20-day average of the horizontal structure of the MJO-like system in Grabowski (2001): a) Zonal flow at 2 km; b) zonal flow at 12 km; c) vertical vorticity at 2 km; and d) vertical vorticity at 12 km. Right, 20-day average of the vertical structure at the equator: a) vertical velocity; b) zonal velocity; c) surface precipitation; and d) surface pressure. Sketched in red are characteristic trajectories. Flow is relative to the MJO-like system. [From Moncrieff (2003).]

4. Nonlinear two-scale analytic model

The general analytic model of the coupled system is defined by six dimensionless quantities: two convective Richardson numbers (mesoscale parameterization), two generalized inverse Rossby numbers (large-scale circulation), and two quantities E_m and E_l that represent the propagation speeds of the organized mesoscale systems and the large-scale circulation, respectively. The latter two quantities are the eigenvalues of the nonlinear steady system. The general model reduces to archetype in which E_m and E_l are the sole dimensionless quantities. This brutal simplification judiciously represents the salient properties of organized convection. Remarkably, the reduced models explain key properties of the large-scale convective organization numerically simulated by G01.

The red flow trajectories in Fig. 4b correspond to the red trajectories in the vertical plane through the equator in Fig. 5. This analytic mesoscale parameterization represents the collective effects of numerous organized convective systems. The quasi-horizontal flow in Fig 4b is idealized in Fig. 5 as a two-layer model of the lower- and upper-tropospheric dynamics shown in Fig. 4b. The dynamics of the lower-layer is Rossby-gyre-like (basically, rotational balance) whereas the upper-layer dynamics is driven by organized outflow from the mesoscale parameterization (basically, divergent balance).

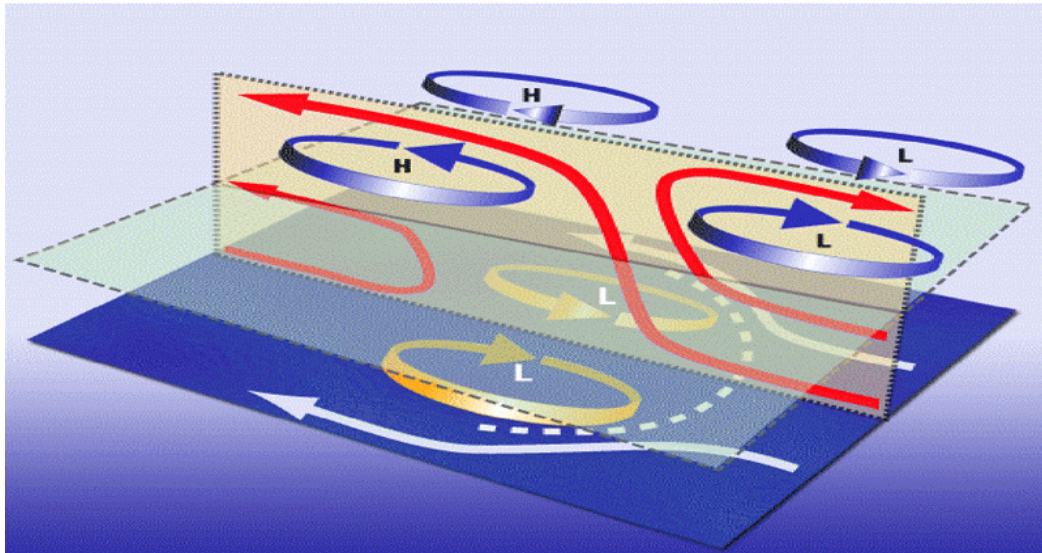


Figure 5: Nonlinear analytic model of mature MJO-like systems formed by coupling a mesoscale parameterization of organized convection (M92) to a two-layer large-scale equatorial beta-plane model. Red trajectories represent the mesoscale parameterization in the vertical plane at the Equator. Yellow trajectories represent a Rossby-gyre-like gyre (rotationally-balanced dynamics) in the lower layer. Blue trajectories are driven by organized outflow from the mesoscale parameterization (divergent-flow balance) in the upper layer. The aspect ratio (horizontal scale/vertical scale) is about 500, so the coupled system is quasi-horizontal.

The flow trajectories in both the horizontal and vertical planes in Fig. 5 are formally represented by the canonical regimes sketched in Fig. 6. For example, the two-branch regime represents the horizontal white trajectories in the lower-layer of Fig 5, and the three-branch regime the mesoscale parameterization (red arrows). The eigenvalues, defined as the quotient of the cross-system pressure change and the kinetic energy of propagation, represent the mesoscale parameterization (E_m) and the large-scale circulation (E_l).

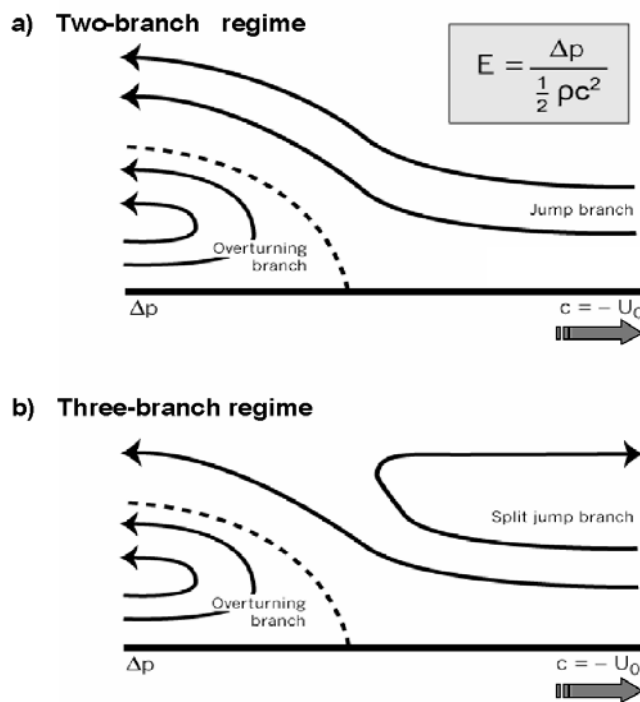


Figure 6: Canonical regimes of organization. a) Two-branch; b) three-branch.

After scaling, the dynamics of the mesoscale parameterization *and* the large-scale circulation are represented by the same dimensionless equations. The solutions of these equations are functions of the eigenvalue of the mesoscale parameterization, ($E_m = \Delta p_m / \frac{1}{2} \rho c_m^2$) and the eigenvalue of the large-scale circulation ($E_l = \Delta p_l / \frac{1}{2} \rho c_l^2$), respectively. Clearly, the propagation speed formulae differ deeply from linear-wave theory, being of the form $c = \sqrt{\frac{2\Delta p}{\rho E}}$, where c is the propagation speed relative to the surface wind.

M92 derived far-field solutions of the nonlinear eigenvalue problem for the mesoscale parameterization in terms of functional relationships among E_m , the depth of the overturning circulation (h) and the depth of the jump inflow (d) in the far-field, valid in the range $-8 \leq E_m \leq \frac{8}{9}$. This solution is plotted in Fig. 7a as well as schema of the regimes of organization for the limit states $E_m = -8, 0, \frac{8}{9}$. For completeness, the corresponding solution for the large-scale circulation is plotted in Fig. 7b.

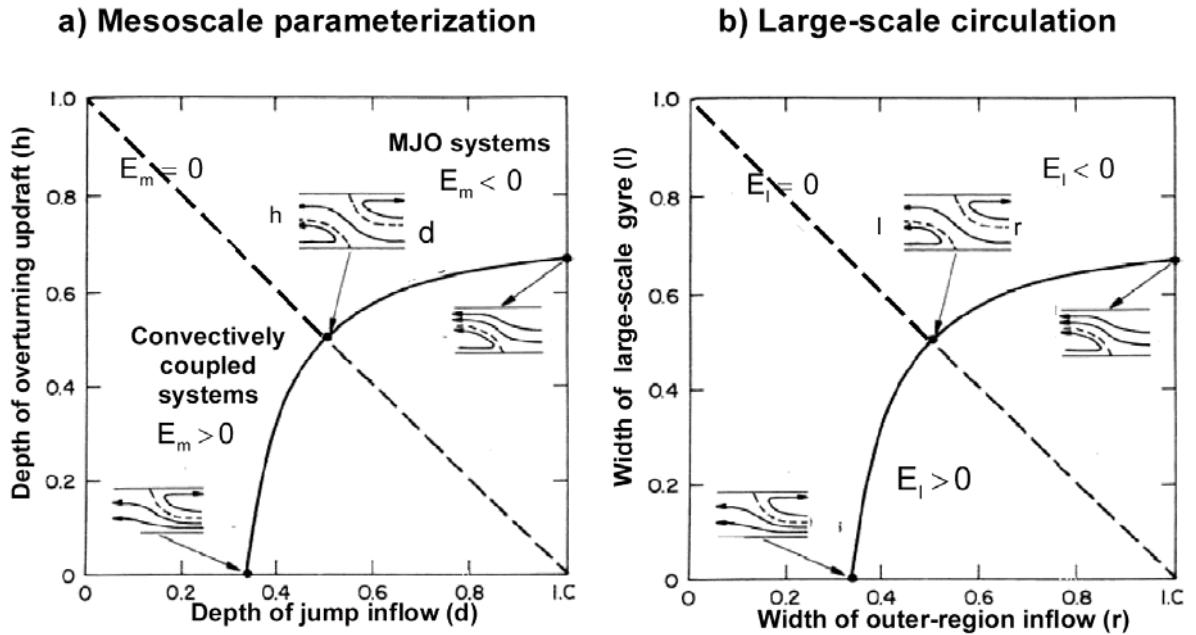


Figure 7: Solutions for the coupled archetypal model. a) Analytic mesoscale parametrizations; b) large-scale circulation. Canonical regimes of organization for each limit state, $E = -8, 0$ and $8/9$ are sketched on the figures.

5. Coupling the mesoscale parameterization to large-scale dynamics

The analytical coupling of the mesoscale parameterization in the vertical plane to the large-scale circulation in the horizontal plane consists of three steps: an interscale morphological analogy and mathematical transformation, a dynamical closure and an integral constraint.

5.1. Inter-scale Transformation

The inter-scale transformation between the mesoscale parameterization and the large-scale circulation is a generalization to a sheared, convecting atmosphere of a classical relationship between gravity waves in unshered constantly stratified flow and Rossby waves on a beta-plane in constant zonal flow.

This analogy is manifested as transformations between the Richardson numbers associated with organized convection and the generalized inverse Rossby numbers associated with the large-scale circulation, and the transformation $E_m \rightarrow E_l$. Only the latter is needed for the archetypal model.

5.2. Dynamical closure

The mesoscale parameterization and the large-scale circulations are related through the propagation speeds (c_m and c_l), and therefore the eigenvalues E_m and E_l are functionally related. Figure 8 identifies two scenarios. Firstly, the mesoscale parameterization retrogresses relative to the large-scale circulation (Fig. 8a), which occurs in the real-world (Nakazawa 1988) and in fully explicit numerical simulations (Grabowski and Moncrieff 2001). Secondly, in the stationary scenario (Fig. 8b) the mesoscale parameterization and the large-scale circulation travel at the same speed, share the same surface front, the inflows have the same kinetic energy: completely interlocked coherent structures.

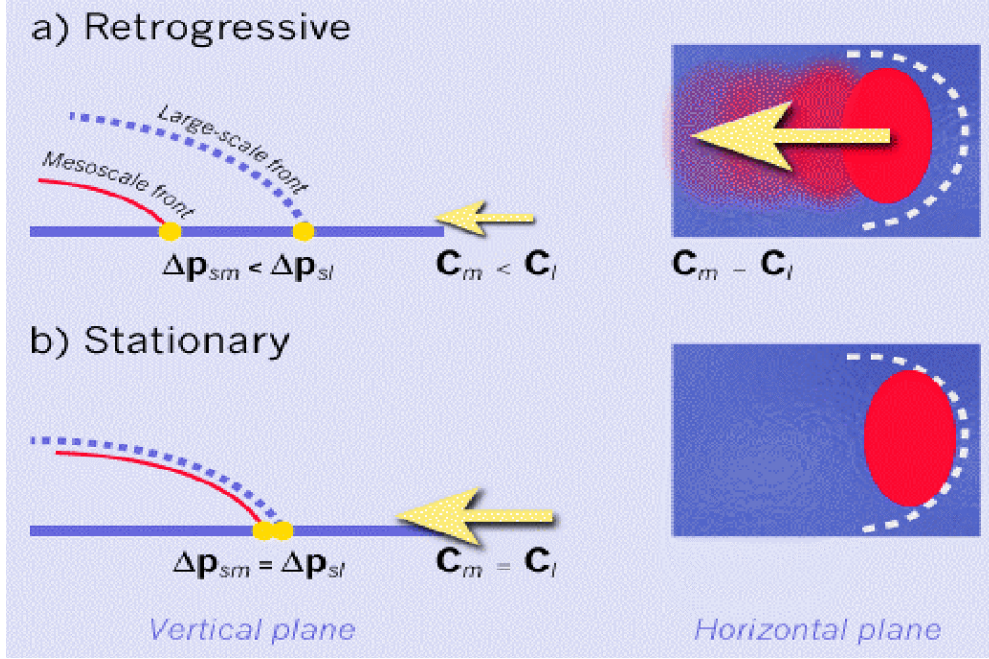


Figure 8: Dynamical closure scenarios in which the mesoscale parameterization: a) retrogresses relative to the large-scale circulation; b) moves at the same speed.

5.3. Integral constraint

The powerful integral constraint is the volume-integral of the horizontal momentum equations for the two scales of motion together with mass-continuity and pressure-continuity and energy-conservation at the (free) boundaries that divide the flow branches. As shown in M92 this refines the eigenvalue (or characteristic) equation, whose solution determines E_m and E_l and the flow morphology (Fig. 7).

6. Evaluation of the analytic model against explicit convection

The proneness of the transport of zonal momentum in the vertical and horizontal directions to error (even in algebraic sign) means momentum transport is a strict test of the coupled analytic model. M92 showed that the total transport of zonal momentum in the vertical direction by the mesoscale parameterization is given by

$$\Lambda_m(z) = - \int_0^z \Upsilon_m(z') dz'$$

where $\Upsilon_m(z) = -\Delta(\rho u_m^2 + p_m)$ and Δ is the standard difference operator. The horizontal momentum flux ρu_m^2 and the pressure distribution p_m at the lateral boundaries are provided by the far-field solutions.

Because the characteristic equation is derived from the volume integral of the horizontal momentum equation, it is assured that $\Lambda_m = 0$ at the upper boundary ($z = 1$), in scaled units.

By analogy, the total meridional transport of zonal momentum is

$$\Lambda_l(y) = - \int_0^y \Upsilon_l(y') dy'$$

where $\Upsilon_l(y) = -\Delta(\rho u_l^2 + p_l)$. Again, the horizontal momentum flux ρu_l^2 and the pressure p_l at the lateral boundaries are given by the far-field solutions and the momentum flux is zero at the poleward boundaries of the beta-channel.

The mesoscale and large-scale momentum transports, which are respective functions of E_m and E_l are now compared to results from G01's explicit convection. Considering the surface pressure gradient in Fig. 4, negative values of E_m are relevant for the mesoscale parameterization (i.e., $-8 \leq E_m \leq 0$). The propagating solution, which is associated with a degenerate overturning branch, occurs when $E_m = -8$, $d = 1$ and $h = 2/3$. The value estimated from G01 is $E_m = -4.7$

Figure 9 compares the meridional momentum transport for $E_l = 0$ and $E_l = -8$. These limit states bound the solution. The 'kink' in the analytic meridional transport of momentum in the neighborhood of the equator results from the fully open gyre of the analytic model (Fig. 6) compared to the closed asymmetric gyre in G01. (The open gyre is a convenient measure of zonal asymmetry that is fundamental to the momentum transport.).

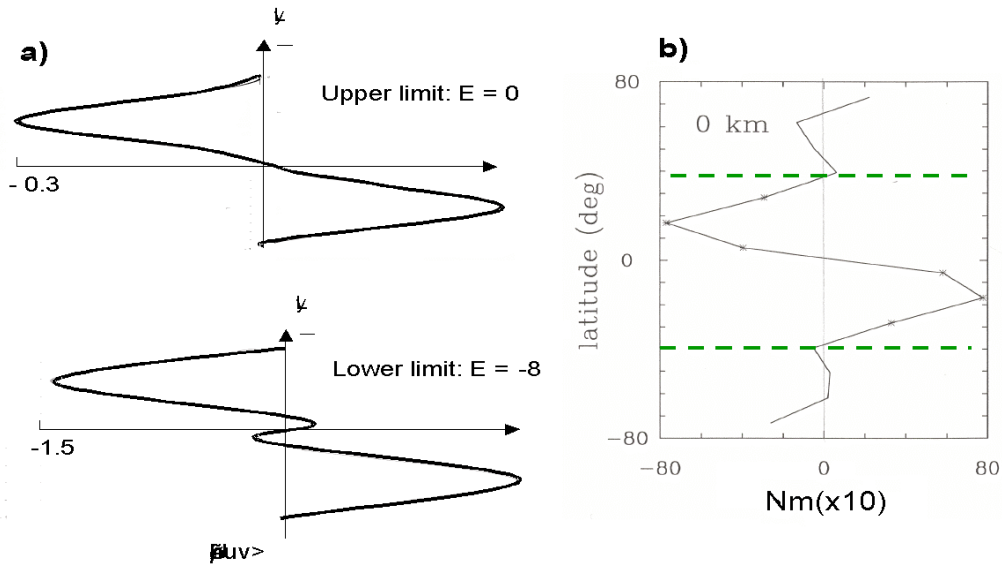


Figure 9: Meridional transport of zonal momentum for the MJO-like system at the ocean surface. a) Analytic model in scaled units, b) results from G01.

Figure 10 compares the vertical transport of zonal momentum. The mostly negative momentum transport is a fundamental property of eastward-traveling mesoscale systems (M92). The shallow positive flux derives from the rearward overturning circulation associated with the westerly wind burst. The vertical transport of momentum in MJO-like systems resembles squall-line transport (M92). This was anticipated because the mesoscale parameterization is supposed to represent the collective effects of numerous squall lines.

The analytic model explains other key dynamical properties features of G01, such as equatorial super-rotation (M03).

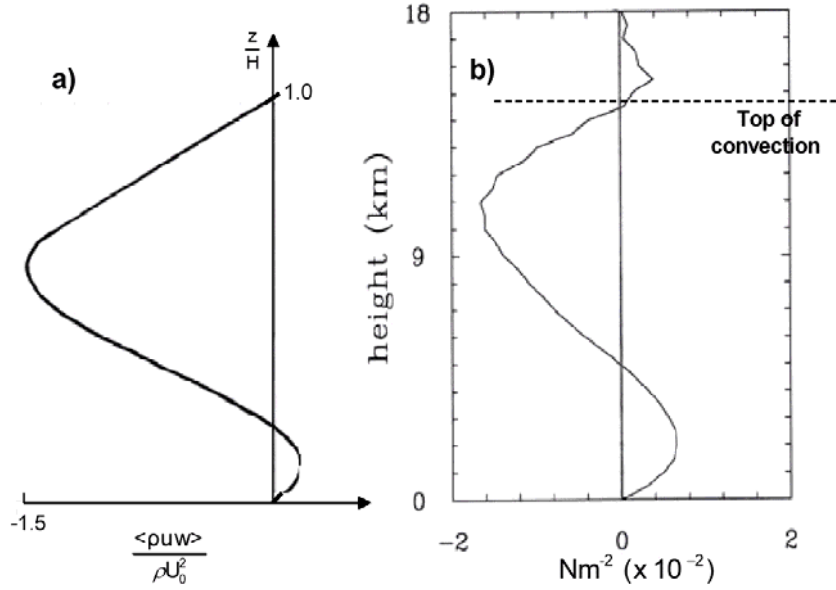


Figure 10: Vertical transport of zonal momentum. a) Analytic model in scaled units, b) results from G01.

7. Concluding remarks

The large-scale role of precipitating convection organized on meso- β -scales in the large-scale organization of tropical convection was quantified by nonlinear dynamical models and inter-scale transformations. Explicit three-dimensional MJO-like systems in G01 are modeled analytically as two interlocked two-dimensional coherent circulations. One parameterizes the mesoscale organization of precipitating convection, the other is a two-layer model of the large-scale tropical coherence.

The lower-layer circulation is Rossby-gyre-like, whereas the upper-layer circulation is driven by organized outflow from the mesoscale parameterization (mesoscale transport of zonal momentum). An archetype of the general model explains the numerically simulated large-scale convective organization, meridional and vertical transport of zonal momentum and equatorial super-rotation. It explains significant aspects of, and was verified against, the large-scale organization of convection in G01.

Key points and hypotheses:

- The nonlinear mechanism of MJO propagation differs deeply from linear-wave theory.
- Rossby-gyre-like dynamics dominates in the lower troposphere whereas outflow from organized convection drives the large-scale circulation in the upper troposphere.
- The analytic parameterization shows that organized convection could be, in principle, represented in convective parameterizations.
- The mesoscale parameterization is an analytic counterpart of explicit convection and thus a physical basis for the explicit (super-parameterization) approach.

Key questions:

- Does surrogate small-scale/cumulonimbus convection distort the explicit results?
- Does super-parameterization exaggerate the effects of organized convection (i.e., two-dimensionality, surrogacy)?

- Does the scale-gap between the cloud-system-resolving models and the coarse-mesh model bias scale selection?
- What is the consistent initial-value problem (i.e., scale-selection principle) for the steady organized convection?

These points, hypotheses and questions need to be addressed by careful evaluation of models against real-world systems, by performing three-dimensional fully explicit numerical simulations, and further mathematical analysis.

Acknowledgements

Support of NASA award NAG5-12010 and the NCAR Clouds in Climate Program (CCP) are acknowledged. The National Center for Atmospheric Research is operated by the University Corporation for Atmospheric Research under sponsorship of the National Science Foundation.

References

- Gill, A. E., 1980: Some simple solutions for heat-induced tropical circulation. *Quart. J. Roy. Meteor. Soc.*, **106**, 447-462.
- Grabowski, W.W., 2001: Coupling cloud processes with the large-scale dynamics using the Cloud-resolving Convection parameterization (CRCP). *J. Atmos. Sci.*, **58**, 978-997.
- Grabowski, W.W., and M.W. Moncrieff 2001: Large-scale organization of tropical convection in two-dimensional explicit numerical simulations. *Quart. J. Roy. Meteorol. Soc.*, **127**, 445-468.
- LeMone, M.A., and M. W. Moncrieff, 1993: Momentum and mass transport by convective bands: Comparisons with highly idealized dynamical models to observations. *J. Atmos. Sci.*, **51**, 281-305.
- Majda, A.J., and R. Klein, 2003: Systematic multiscale models for the Tropics. *J. Atmos. Sci.*, **60**, 393-408.
- Matsuno, T., 1966: Quasi-geostrophic motions in the equatorial area. *J. Met. Soc. Japan*, **44**, 25-43.
- Moncrieff, M.W., 1992: Organized convective systems: archetypal dynamical models, mass and momentum flux theory, and parameterization. *Quart. J. Roy. Meteorol. Soc.*, **118**, 819-950.
- Moncrieff, M.W., 2003: Analytic representation of the large-scale organization of tropical convection. *J. Atmos. Sci.*, in press.
- Moncrieff, and E. Klinker, 1997: Mesoscale cloud systems in the Tropical Western Pacific as a process in general circulation models. *Quart. J. Roy. Met. Soc.*, **123**, 805-827.
- Nakazawa, T., 1988: Tropical superclusters within intraseasonal variations over the western Pacific. *J. Meteor. Soc. Japan*, **66**, 823-839.
- Slingo, J.M., and Co-authors, 1996: Intraseasonal oscillations in 15 atmospheric general circulation models: Results from an AMIP diagnostic subproject. *Clim. Dyn.*, **12**, 325-357.
- Sobel, A.H., J. Nilsson, and L. M. Polvani, 2001: The weak temperature gradient approximation and balanced tropical moisture waves. *J. Atmos. Sci.*, **58**, 3650-3665.
- Sperber, K.R., J.M. Slingo, P. K. Inness, and K.-M. Lau, 1997: On the maintenance and initiation of the intraseasonal oscillation in the NCEP/NCAR reanalysis and in the GLA and UKMO AMIP simulations. *Clim. Dyn.* **13**, 769-795.
- Webster, P.J., 1972: Response of the tropical atmosphere to local steady forcing. *Mon. Wea. Rev.*, **100**, 518-541.